
Traversing Geodesics to Grow Biological Structures

Anonymous Author(s)

Affiliation

Address

email

Abstract

1 Biological tissues reliably grow into functional structures from simple starting
2 states during development. Throughout this process, the energy of a tissue changes
3 depending on its natural resistance to deformations such as stretching, bending,
4 shearing, and torsion. In this paper, we represent tissue structures as shapes and
5 develop a mathematical framework to discover paths on the tissue shape manifold
6 to minimize the total energy during development. We find that paths discovered by
7 gradient descent and the geodesic algorithm outperform naive shape interpolation
8 in energetic terms and resemble strategies observed in development. Broadly, these
9 tools can be used to understand and compare shape transformations in biology and
10 propose optimal strategies for synthetic tissue engineering.

11 1 Introduction

12 In biological tissues, shape and function are inextricably linked. For instance, the intricate architecture
13 of the heart allows it to efficiently deliver oxygenated blood to the body. During cardiac development
14 (cardiogenesis), a single population of early precursors fuses into the primitive heart tube and must
15 undergo a series of precise loopings, rotations, and partitions, while simultaneously functioning as a
16 pump [1]. As a result, congenital heart malformations [2, 3] are the most common fatal birth defects
17 in infants, for whom birth defects are the number one cause of death. Of the many possible paths from
18 an initial form to a final form, why do biological tissues transform in the manner as observed? From
19 the perspective of physics, as a tissue changes shape, it traverses an energy landscape determined by
20 its natural resistance to deformations from a resting state.

21 To better understand this problem, we design a mathematical approach inspired by AI to discover
22 minimum-energy strategies for growing a folded rigid tubular structure from an initially round tissue.
23 We generate candidate paths for this simple morphological operation using naive interpolation, an
24 algorithm for geodesic (locally low-energy) paths, and gradient descent. We find that geodesic and
25 gradient descent paths open up the tissue at the opposite end from the site of folding, thus bypassing
26 closed intermediates with high tensile energy. Broadly, our work supplies tools for understanding
27 biological development and discovering novel strategies for synthetic tissue engineering.

28 2 Mathematical framework

29 2.1 Preliminaries

30 In our mathematical framework adapted from [4, 5], we represent an organic structure as a 2-
31 dimensional shape, wherein the sampled coordinates of the shape are vertices of the shape manifold
32 $(S) = \mathbb{R}^{m \times 2}$, where m is the number of vertices and ‘2’ refers to the 2 axes x and y . In addition, we
33 define an energy function $(E(s) = \mathbb{R}^n)$, that maps an organic structure s to the energy space (E) .
34 The energy space is a vector in \mathbb{R}^n , where the n elements correspond to n separable energies, whose
35 relative contributions can be balanced based on the properties of the tissue being examined. In this

36 work, we approximate a rigid tissue as a covalent solid, or a network of stretchable bonds connected
 37 by bendable joints. Thus, a shape's energy is the sum of the stretching and bending energies of its
 38 constituent bonds and joints (Fig. 1A).

$$E(s, t) = \begin{bmatrix} E_{\text{stretch}} \\ E_{\text{bend}} \end{bmatrix} = \begin{bmatrix} B \sum_{i=0}^{m-1} (\ell_i - \ell_i^{(0)}(t))^2 \\ K \sum_{i=0}^{m-2} (\theta_i - \theta_i^{(0)}(t))^2 \end{bmatrix} \quad (1)$$

39 Here, B and K are the stretching and bending moduli (analogous to a material's bulk modulus and
 40 bending rigidity). The stretching energy is the spring potential for a spring described by the vector
 41 $\mathbf{r}_j = s_{j+1} - s_j$ with resting length $\ell_j^{(0)}(t)$, and the bending energy is the harmonic angle potential for
 42 the signed bending angle between \mathbf{r}_j and \mathbf{r}_{j+1} with resting angle $\theta_j^{(0)}(t)$. Spring lengths and bending
 43 angles were calculated as

$$\ell_j = \|\mathbf{r}_j\|_2, \quad \theta_j = \text{Sgn}(\mathbf{r}_j \times \mathbf{r}_{j+1}) \arccos\left(\frac{\mathbf{r}_j \cdot \mathbf{r}_{j+1}}{\|\mathbf{r}_j\|_2 \|\mathbf{r}_{j+1}\|_2}\right), \quad (2)$$

44 where Sgn is the signum operator.

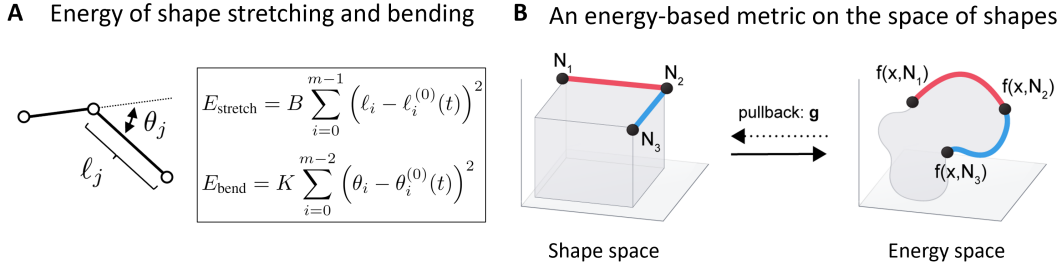


Figure 1: (A) Energy of a structure is evaluated by modeling the bonds as a flexible network of nodes with pre-defined resting lengths and angles. (B) Geometric framework for growing biological structures. Three biological structures (N_1, N_2, N_3) in shape space \mathcal{S} and their relative distance in the Energy space. Growth of biological structures is analyzed by asking how movement in shape space changes the energy through introduction of a pullback metric \mathbf{g}

45 **Objective:** Our goal is to find a path ($\gamma(t)$) between two organic structures ($\mathbf{s}_1, \mathbf{s}_f \in \mathcal{S}$) while
 46 optimizing relevant energy terms, based on the developmental process being modeled.

47 2.2 Metric Tensor construction

48 To formalize the notion of energy change as the structure (2D shape) changes, we evaluate how
 49 infinitesimal perturbation in the shape manifold (\mathcal{S}) impacts movement in the energy space (\mathbf{E}) by
 50 constructing a metric tensor (Fig 2B). To construct the metric, we ask how the energy changes (\mathbf{E}) as
 51 the 2D shape is infinitesimally changed from $\mathbf{s}_1 \in \mathcal{S}$ by $d\mathbf{s}$.

$$E(\mathbf{s}_1 + d\mathbf{s}) \approx E(\mathbf{s}_1) + \mathbf{J}_{\mathbf{s}_1} d\mathbf{u}, \quad (3)$$

52 where $\mathbf{J}_{\mathbf{s}_1}$ is the Jacobian of $E(\mathbf{s}_1)$ and $J_{i,j} = \frac{\partial E_i}{\partial s_j}$, evaluated at \mathbf{s}_1 .

53 In this work, we evaluate the change in energy ($d_E(d\mathbf{s}, \mathbf{g}_{\mathbf{s}_1})$) by calculating the Euclidean distance
 54 between the energy vectors corresponding to shapes \mathbf{s}_1 and $\mathbf{s}_1 + d\mathbf{s}$. (Please note that general
 55 (non-Euclidean) distance measures can be constructed on the output space, but we focus on the
 56 Euclidean case for clarity).

$$d_E(d\mathbf{s}, \mathbf{g}_{\mathbf{s}_1}) = \sqrt{|E(\mathbf{s}_1 + d\mathbf{s}) - E(\mathbf{s}_1)|^2} = \sqrt{d\mathbf{s}^T (\mathbf{J}_{\mathbf{s}_1}^T \mathbf{J}_{\mathbf{s}_1}) d\mathbf{s}} = \sqrt{d\mathbf{s}^T \mathbf{g}_{\mathbf{s}_1} d\mathbf{s}} \quad (4)$$

$$d_E(d\mathbf{s}, \mathbf{g}_w) = \sqrt{d\mathbf{s}^T \mathbf{g}_w d\mathbf{s}} \quad (5)$$

57 where $\mathbf{g}_{\mathbf{s}_1} = \mathbf{J}_{\mathbf{s}_1}^T \mathbf{J}_{\mathbf{s}_1}$ is the metric tensor evaluated at the point $\mathbf{s}_1 \in \mathcal{S}$ and $d_E(d\mathbf{s}, \mathbf{g}_s)$ is the
 58 distance moved in output space when the weights are perturbed by $d\mathbf{s}$ at $\mathbf{s} \in \mathcal{S}$.

59 2.3 Constructing minimal energy paths in the shape manifold

60 Our objective is to find a path in the shape manifold (\mathcal{S}) between two 2D shapes (\mathbf{s}_1 and \mathbf{s}_2),
 61 representing biological tissue structures at separated time-intervals during the developmental process
 62 (as shown in Fig. 2A), such that the total energy consumed during the transformation is minimized.

63 Mathematically, we want to find a curve $\mathcal{C} \in \mathcal{S}$, with start and end points \mathbf{s}_1 and \mathbf{s}_2 respectively, such
 64 that the integrated energy of the transformation is minimized.

$$L(\mathcal{C}) = \int_{\mathcal{C}} d_E(\mathbf{ds}, \langle \mathbf{g}_w(\mathbf{x}) \rangle) \quad (6)$$

$$= \int_{\mathcal{C}} \sqrt{\mathbf{ds}^T \langle \mathbf{g}_s \rangle \mathbf{ds}} \quad (7)$$

On parameterizing the curve traversed ($\mathcal{C} \in \mathcal{S}$) by $\gamma : [0, 1] \rightarrow \mathcal{S} \in W$, wherein $\gamma(0) = \mathbf{s}_1$,
 $\gamma(1) = \mathbf{s}_2$, the differential element along the path (\mathbf{ds}) can be rewritten as:

$$\mathbf{ds} = \frac{d\gamma}{dt} dt, \quad \mathbf{s} = \gamma(t)$$

65 The total length of the path parameterized by $\gamma(t)$ is:

$$L(\gamma) = \int_0^1 \sqrt{\left(\frac{d\gamma}{dt}(dt)\right)^T \langle \mathbf{g}_{\gamma(t)}(\mathbf{x}) \rangle \left(\frac{d\gamma}{dt}(dt)\right)} \quad (8)$$

$$L(\gamma) = \int_0^1 \sqrt{\frac{d\gamma(t)}{dt}^T \langle \mathbf{g}_{\gamma(t)} \rangle \frac{d\gamma(t)}{dt}} dt, \quad (9)$$

66 Let Ω be the set of all piecewise differentiable curves from \mathbf{s}_1 to \mathbf{s}_2 in the shape manifold (\mathcal{S}), we
 67 want to find γ^* such that:

$$L(\gamma^*) = \min_{\gamma} L(\gamma) \quad \forall \gamma \in \Omega \quad (10)$$

68 Therefore, minimizing $L(\gamma)$ enables the discovery of low-energy paths in the shapes manifold between
 69 two shapes, corresponding to biological structures at different stages of development. We find the
 70 geodesic path from the source to the target shape by applying the path-straightening approach [6, 7].
 71 The algorithm is seeded with the linear path as the starting path, and the shapes along the linear path
 72 are adjusted in order to minimize the total energy of the path.

73 3 Results

74 We seek to study how cells and tissues traverse the energy landscape between disparate "source"
 75 and "target" structures. During development, the same tissue structure is often generated in different
 76 ways depending on the developmental context, suggesting the existence of multiple paths in the
 77 energy landscape with different energetic trade-offs. For instance, a tube is a fundamental unit of
 78 many tissues and organs, and yet tubes form in a variety of ways, including wrapping, budding,
 79 and hollowing/cavitation [8]. Let us consider growing a tube from a rigid aggregate of uniform,
 80 adhesive cells. Initially, the tissue would adopt a spherical configuration due to surface tension. Two
 81 mechanisms for tube-formation, wrapping and budding, involve creating high positive and negative
 82 curvature on opposing ends of a folding structure, resulting in a wrinkle or dimple. To represent
 83 this process in 2D, we start from a circular source shape and specify a folded target shape (a hollow
 84 annulus prior to fusion of the tube), assuming the tissue is rigid throughout.

85 We assume that this transformation is thermodynamically favorable such that $\lim_{t \rightarrow \infty} \ell_j^{(0)}(t) =$
 86 ℓ_{j, s_2} , $\lim_{t \rightarrow \infty} \theta_j^{(0)}(t) = \theta_{j, s_2} \quad \forall j$. As in development, the tissue will eventually relax to its target
 87 shape in the absence of external forces. We begin with the simple case where resting lengths and
 88 angles are constant ($\ell_j^{(0)} = \ell_{j, s_2}$ and $\theta_j^{(0)} = \theta_{j, s_2}$).

89 We first generate a naive path by linearly interpolating Cartesian coordinates for each point in the
 90 shape (Fig 2A, top). In this naive path, the source shape gradual involutes on the bottom side and
 91 stretches on the top in order to fold into the target shape, remaining closed throughout. We then apply

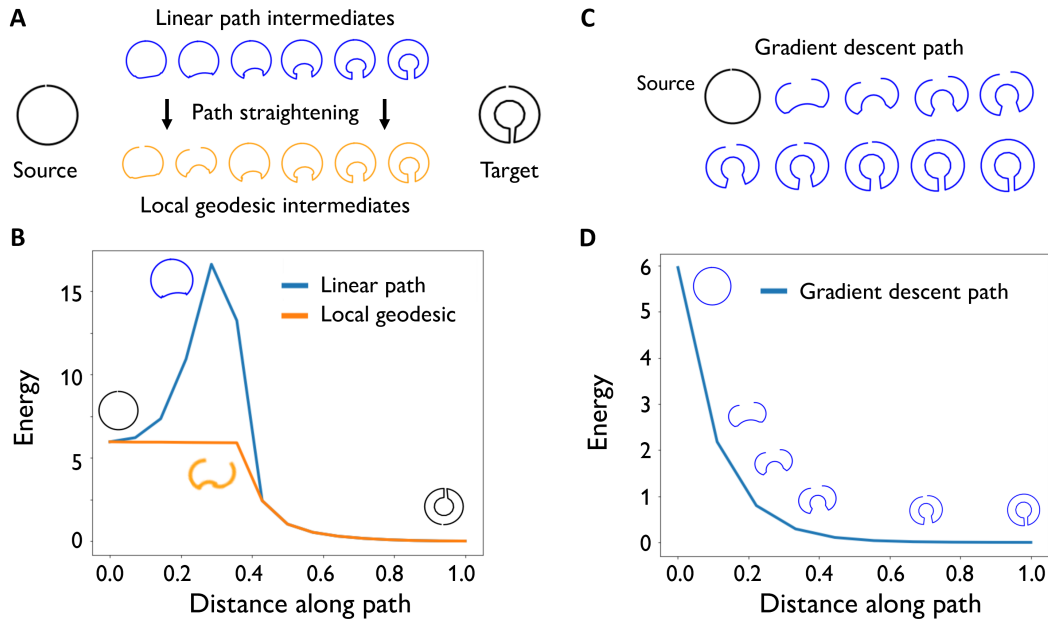


Figure 2: (A) Source and Target shape as we move in the shape manifold. Path Straightening algorithm finds the local Geodesic beginning from the linear path in the shape space. (B) Geodesic path minimizes the energy of the path between source and target structures. (C) Gradient descent minimization of the energy of the source shape, discovers a string of open-networks before converging at the target shape. (D) The energy along the path that traverses the gradient of the energy function is demonstrated here.

92 a path straightening algorithm to the linear path. The resulting local geodesic path involves a sudden
 93 opening of the structure (Fig. 2A, bottom). Plotting the energy along both paths (Fig. 2B) reveals
 94 that the unfolding intermediate corresponds to the highest-energy shape in the linear path, suggesting
 95 that the geodesic is bypassing an energy barrier during involution. We further find that a gradient
 96 descent algorithm applied to the source shape generates a path that similarly opens up the structure,
 97 allowing the right and left arms to move independently as it converges to the target (Fig. 2CD).

98 We hypothesize that as involution occurs at one end of the tissue, the other end must transiently
 99 stretch in order to preserve a closed configuration. The geodesic and gradient descent paths avoid this
 100 high-energy intermediate by transiently opening the structure topology. This result highlights the
 101 potential for mechanical forces to exert long-range effects in development, whereby morphological
 102 events seemingly isolated to one region of an embryo can in fact be enabled by changes occurring in
 103 distant regions [9].

104 4 Discussion

105 Our preliminary experiments suggest that we can use structural modeling and a mathematical
 106 framework to find energy-efficient paths between biological structures that avoid energy barriers
 107 encountered by naive shape interpolation. Because each path provides a program for each element of
 108 the biological tissue to follow, they can be seen as a set of cell-level instructions for transforming a
 109 biomaterial as a whole. Such instruction sets could be useful for the engineering of a next generation
 110 of synthetic lab-grown tissues with defined morphology.

111 This approach also could be extended in order to reverse-engineer the material properties (energy
 112 function parameters) of a developing/deforming tissue by minimizing the distance between experi-
 113 mental and model-predicted shape trajectories. This method would enable measurement of a tissue's
 114 material properties in a much less invasive fashion than current methods and with greater spatial and
 115 temporal resolution.

116 **References**

- 117 [1] Kenneth R Chien, Ibrahim J Domian, and Kevin Kit Parker. “Cardiogenesis and the complex
118 biology of regenerative cardiovascular medicine”. In: *Science* 322.5907 (2008), pp. 1494–1497.
- 119 [2] Cheryl S Broussard et al. “Racial/ethnic differences in infant mortality attributable to birth
120 defects by gestational age”. In: *Pediatrics* 130.3 (2012), e518–e527.
- 121 [3] JR Petrini et al. “Racial differences by gestational age in neonatal deaths attributable to congeni-
122 tal heart defects-United States, 2003-2006.” In: *Morbidity and Mortality Weekly Report* 59.37
123 (2010), pp. 1208–1211.
- 124 [4] Guruprasad Raghavan and Matt Thomson. “Solving hybrid machine learning tasks by traversing
125 weight space geodesics”. In: *arXiv preprint arXiv:2106.02793* (2021).
- 126 [5] Guruprasad Raghavan, Jiayi Li, and Matt Thomson. “Geometric algorithms for predicting
127 resilience and recovering damage in neural networks”. In: *arXiv preprint arXiv:2005.11603*
128 (2020).
- 129 [6] Qian Xie et al. “Parallel transport of deformations in shape space of elastic surfaces”. In:
130 *Proceedings of the IEEE International Conference on Computer Vision*. 2013, pp. 865–872.
- 131 [7] Keenan Crane et al. “A Survey of Algorithms for Geodesic Paths and Distances”. In: *arXiv*
132 *preprint arXiv:2007.10430* (2020).
- 133 [8] Barry Lubarsky and Mark A Krasnow. “Tube morphogenesis: making and shaping biological
134 tubes”. In: *Cell* 112.1 (2003), pp. 19–28.
- 135 [9] Farid Alisafaei et al. “Long-range mechanical signaling in biological systems”. en. In: *Soft*
136 *Matter* 17.2 (Jan. 2021). Publisher: The Royal Society of Chemistry, pp. 241–253. ISSN:
137 1744-6848. DOI: 10.1039/D0SM01442G. URL: [https://pubs.rsc.org/en/content/
138 articlelanding/2021/sm/d0sm01442g](https://pubs.rsc.org/en/content/articlelanding/2021/sm/d0sm01442g) (visited on 09/22/2021).